ARTICLE

Characterization and performance test of phenolphthalein poly(aryl ether ketone) fractionated by incremental poor solvent fractionation

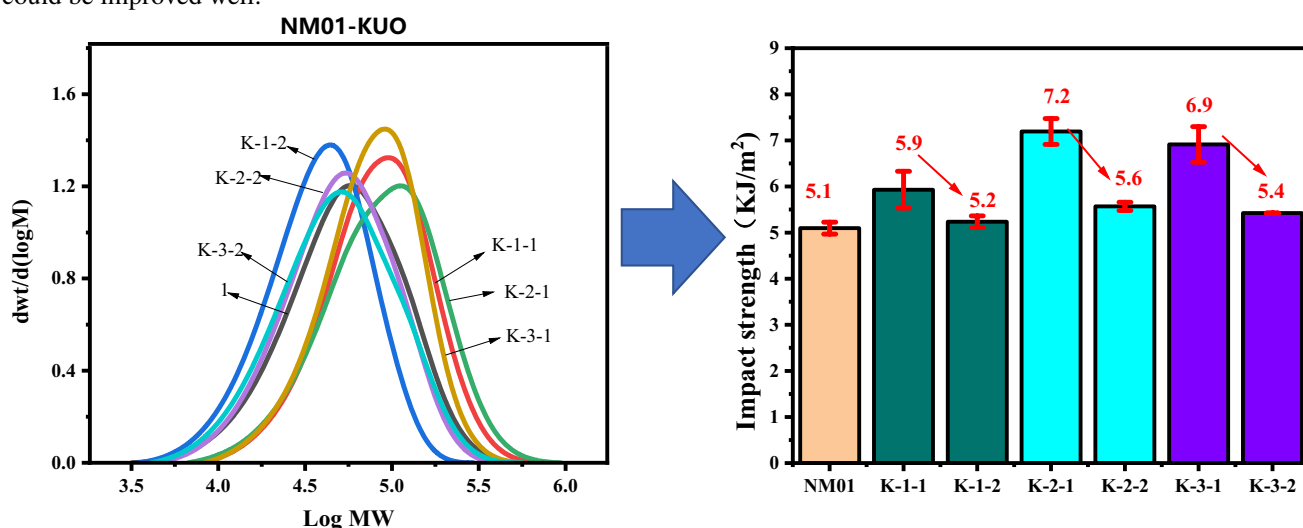Zengxu Qian[1] · Jingwei Jiang[1] · Yunlong Sun[2] · Qiliang Yuan[3] · Zhichao Wang[1] · Zhipeng Wang[2] · Guangyuan Zhou[2]

Abstract

Though phenolphthalein poly(aryl ether ketone) (PEK-C) has gained attention as a special engineering plastic materials by virtue of its good thermal stability and favorable mechanical properties, its applications are limited due to its wide PDI during polymerization, which result in poor mechanical properties of PEK-C. In order to investigate the effect of molecular weight and polydispersity index (PDI) on PEK-C, an incremental poor solvent fractionation method was used to fractionate PEK-C. The process produced a series of grades with decreasing molecular weight and PDI. The LCP (linear cloud point) equation was combined with the grading method to find the optimal PEK-C/DMAc/ Non-solvent additives (NSA) system, which can be used to improve the grading efficiency. The obtained results showed that the incremental poor solvent fractionation method with the PEK-C/DMAc/EA system made the molecular weight distributed in the range of 25 ~ 113 kDa, PDI mostly distributed in the range of 1.1 ~ 1.4, and the narrowest PDI to reach 1.13, which could not be obtained through the condensation reaction. Meanwhile, we can also achieve expanded production. By fractionation, the elastic modulus of PEK-C film could be increased by up to 22.6%, elongation at break by up to 38.3%, the fracture strength by up to 38.2%, and impact strength of the sheest by up to 41.2%, while the polymer still maintained good thermal and UV shielding properties. This unique Polymer/Solution/NSA system can yield an effective design strategy for controlling its molecular weight and PDI and improving its mechanical performance.

Graphical abstract

PEK-C (NM01) was fractionated by incremental poor solvent fractionation. Due to the weak pr ecipitation strength of EA to PEK-C, a large number of grades can be obtained by expanding the classification. Through the method of adding precipitant, NM01 was fractionated into two parts with different molecular weights and PDIs. The impact strength of these grades could be improved well.

Springer

1 Introduction

Molecular weight distribution refers to the degree of dispersion of the molecular weight of a polymer [1]. A polymer actually consists of a mixture of polymers with the same structure and composition, but with different molecular weights. This property of polymers is called polydispersity. In fact, almost physical properties of every polymer are related to its molecular weight and their molecular weight distribution, which have been supported by many experimental results [2–7]. During these experiments, it was found that the molecular weight of a polymer must reach a certain value in order to have a certain mechanical strength. Meanwhile, when the molecular weight of the polymer exceeds a certain level, its mechanical strength does not change a lot, which causes difficulties in its processing [8].

In case of plastics, the molecular weight depends on the requirements of a product, and sometimes it can vary widely [9–12]. However, a narrow PDI is beneficial to its machining performance, as there is a small amount of polymer with low molecular weight that can act as an internal plasticizer [13]. In case of synthetic fibers, a narrow PDI is preferred due to its smaller average molecular weight [14–17]. In case of a wider PDI, it is detrimental to spinning performance and mechanical strength. Accordingly, polymers with narrow PDI are our main target. [18]

As a special engineering plastic, poly(aryl ether ketone) has exhibited excellent performance in many applications, such as high temperature resistance, organic solvent resistance, high strength, and high elastic modulus [19–23]. Phenolphthalein poly(aryl ether ketone) (PEK-C) is an amorphous high-performance thermoplastic having good solubility and excellent processing performance due to the Cardo side group structure in its main molecular chain, which greatly reduces the ordered arrangement of the chain [24–27]. At the same time, compared with polyether ether ketone (PEEK), PEK-C has the same comprehensive performance, making it not only broadly applicable in structural materials but also greatly promising in functional materials. [28–30]

However, when PEK-C is synthesized through the S_N2 aromatic nucleophilic polycondensation reaction, its PDI generally ranges from 1.5 to 3.0 [31, 32]. So, it is difficult to obtain PEK-C with a narrow PDI in order to make it applicable to special fields. At present, there exist many polymer fractionation methods to control molecular weight and PDI, such as precipitation fractionation, dissolution fractionation

and gel permeation chromatography fractionation [33–35]. Li fractionated low density polyethylene resin having high-speed extrusion coating property through the solvent gradient fractionation technique at 115 °C. The obtained fractions showed the molecular weight was increased from 1.58×10^3 Da to 4.76×10^5 Da. The PDI of most fractions were in the range of 1.1–1.2 [36]. Lehtinen found that the fractionation proceeded according to the molecular weight when ethylene glycol monobutyl etheddiethylene glycol monobutyl ether was used as a solvent/non-solvent system at 159–161 °C. The fractions covered a broad range of molecular weights, had narrow PDI, and showed only small variations in their isotacticity [37]. Tan fractionated free radically polymerized broad-distributed HTPB into five narrow-distributed standards by methanol precipitation. The peak shape of self-made HTPB standard sample is symmetrical and narrow, the molecular weight distribution is even, and the dispersion index D is less than 1.3. [38] Choi characterized poly(dimethylsiloxane) (PDMS) by interaction chromatography using C4-bonded silica and THF/CH_3OH mixtures as stationary and mobile phases, respectively. Successfully fractionated according to molecular weight into fractions with a very narrow molecular weight distribution [39]. Unfortunately, these articles do not explore the effect of molecular weight and PDI on polymer properties.

Among these fractionations, only precipitation fractionation is the simplest and most widely used classical fractionation method [40–43]. Besides, only precipitation fractionation has ability to expand production. The basic principle of this method is that with the addition of a poor solvent, the solvation of a homogeneous polymer solution decreases, intermolecular cohesion increases, and the cohesion of a large molecular weight increases. When the threshold is reached, it is precipitated in the order of molecular weights from largest to smallest.

However, the selection of grading systems currently relies on empirical and experimental comparisons only. Their mature theoretical and quantitative relationships have not yet been established. Based on the extended Flory–Huggins theory of polymer solutions, Boom constructed a Polymer/Solution/Non-solvent additive (NSA) system, where a linear correlation function was derived for cloud-point composition curves of ternary system consisting of one polymer, one solvent and one non-solvent [44–49]. The correlation function was derived under the assumptions that the polymer was strongly incompatible with the non-solvent, and only liquid–liquid demixing took place. The linearized cloud-point (LCP) curve was

interpreted in terms of various parameters of the Flory–Huggins theory. The slope of the LCP line was dependent only on the molar volumes of the components. Information about the binary parameters of the Flory–Huggins interaction and their concentration dependencies can be obtained from the intercept of the linearized curve.

In this paper, we propose a process of combining the grading method with the ternary phase diagram to find a suitable PEK-C/DMAc/NSA grading system, which can prepare PEK-C with a narrow PDI. Eventually, we found PEK-C/DMAc/EA system to be the best. Besides, we get 70 g PEK-C with high molecular weight by using the expanded the fractionation method. Futher, GPC, DSC, TGA, and mechanical properties of films and sheets were tested for all grades, in order to investigate the effects of molecular weight of a polymer and PDIon mechanical properties of the polymer.

2 Experimental

2.1 Materials

PEK-C (NM01) was purchased from Zhejiang PAEK New Material Co, Ltd, whose chemical structure is shown in Fig. 1. N, N-dimethylacetamide (DMAc), N, N-dimethylformamide (DMF) and Ethyl acetate (EA) were purchased from Guangdong Guanghua Technology Co, Ltd. Ultra-pure water was self-made in our laboratory. All the purchased chemicals were of an analytical pure grade and used without any further purification.

2.2 Derivation of LCP linear cloud point equation

Due to the local precipitation in high concentration solutions during turbidity titration, it is difficult to obtain the cloud point through experiments. Many researchers proposed empirical or semi-empirical formulas to calculate the turbidity point of a high concentration solution, among which the linear cloud point equation proposed by Boom is widely used [44].
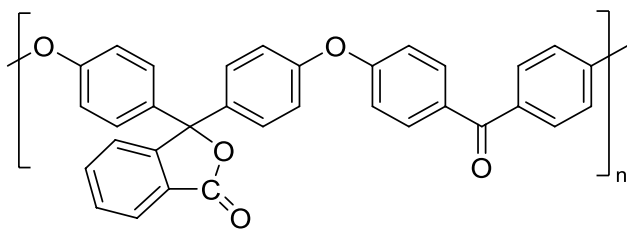
$$ln\frac{F_1}{F_3} = bln\frac{F_2}{F_3} + a \qquad (1)$$

Fig. 1 Chemical structure of PEK-C

In Eq. (1), F_1, F_2 and F_3 are the mass fractions of the poor solvent, solvent and polymer, respectively. The turbidity point of a high concentration solution can be determined by measuring that a low concentration solution.

DMAc was used as a good solvent to prepare the PEK-C solution with different solid concentrations, specifically 1, 1.5, 2, 2.5, and 3%. At a constant temperature of 30 °C, the solution was stirred until the polymer was completely dissolved. Meanwhile, using H_2O, EtOH and EA as solutes, a DMAc solution with a mass fraction of 15% was prepared, and then it was used as the poor solvent additive. Finally it was slowly added to the PEK-C solvent until the solution became cloudy and did not fade within 30 s, at which point the mass fraction of each component was recorded.

2.3 Incremental poor solvent fractionation of PEK-C

Using DMAc as the solvent, PEK-C was prepared as a dilute solution with a weight concentration of 4%. While stirring, the poor solvents (H_2O, EtOH, and EA) were gradually added to make the solution precipitated gradually. After stewing, the upper liquid was poured out and addition of the poor solvent was continued for fractionation. DMAc was added to dilute the highly viscous liquid. Then, it was poured into a mixed solution of EtOH and H_2O, and precipitated during stirring to obtain a white fibrous solid. A white powder was obtained after grinding, washing and drying.

2.4 Characterizations

FT-IR spectra were obtained from a Fourier-transform infrared (IR Tracer-100, Japan) spectrometer to characterize the chemical structure of every grade. The Gel Permeation Chromatography (GPC) was recorded on a Waters 1515 pump with 2414 differential refractive index detector, using narrow polydispersity polystyrene standards in

Table 1 Experimental data on titration of different titrants in PEK-C/DMAc/EA systems

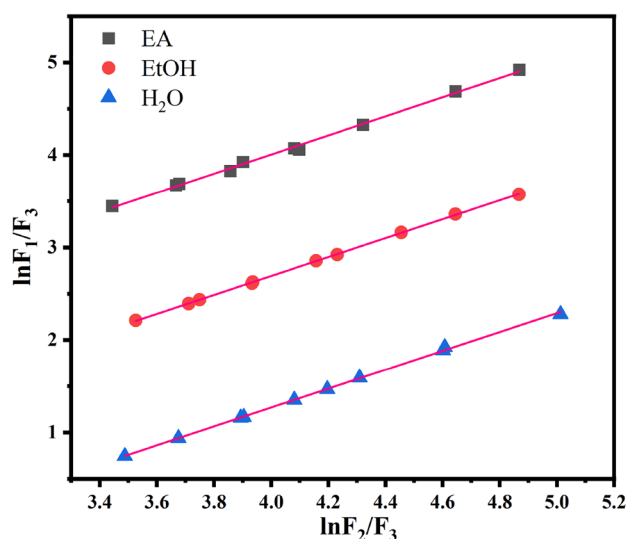| C_{PEK-C} (w/w) (%)	m_{PEK-C} (g)	30 °C		
		H_2O	EtOH	EA
		$m_P:m_S:m_N$		
1.0	0.1916	0.93: 92.74: 6.33	0.75: 77.74: 21.52	0.47: 48.68: 50.86
1.5	0.2889	1.39: 92.57: 6.04	1.13: 77.84: 21.02	0.84: 50.53: 48.63
2.0	0.3871	1.86: 92.18: 5.96	1.52: 77.71: 20.77	1.06: 50.19: 48.75
2.5	0.4864	2.33: 91.74: 5.94	1.89: 77.38: 20.72	1.24: 49.10: 49.66
3.0	0.5867	2.79: 91.33: 5.87	2.27: 77.00: 20.73	1.57: 49.11: 49.32

Fig. 2 Cloud point data of PEK-C/DMAc/NA systems

Table 2 LCP fitting results for cloud point data of PEK-C/DMAc/NA system

Precipitating agent	Temperature (°C)	Fitting equation	Linearly dependent coefficient
H_2O	30	$y = 1.022\ x - 2.817$	$R^2 = 0.999$
EtOH	30	$y = 1.023\ x - 1.4020$	$R^2 = 0.999$
EA	30	$y = 1.033\ x - 0.1278$	$R^2 = 0.997$
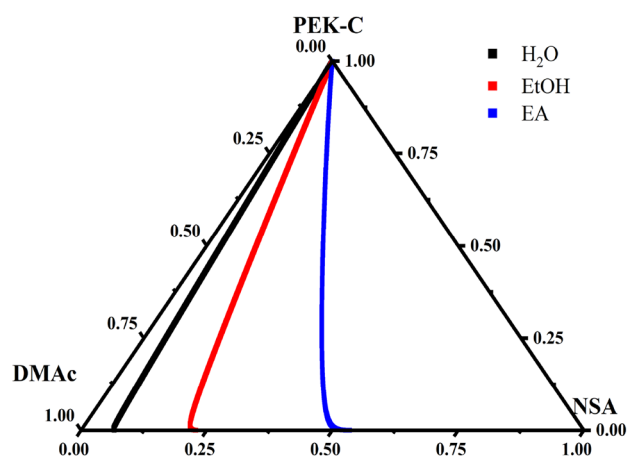
Fig. 3 Cloud point curves of three PEK-C/DMAc/NSA systems at 30 ℃

tetrahydrofuran at 35 °C. The intrinsic viscosity [η] of the polymer was measured by a Ubbelohde viscometer in DMF at 25 °C. The thermogravimetric analysis was performed on TGA55 (TA instrument) in a nitrogen atmosphere from 50 °C to 700 °C with a heating rate of 10 °C/min. The

differential scanning calorimetry curves were obtained with a DSC25 (TA Instruments) from 30 to 350 °C at a heating rate of 10 °C/min under continuous nitrogen flow (40 mL/min). The glass transition temperatures (T_g) were collected from the second heating traces and read at the midpoints of the transitions in the heat flow. The polymers were dissolved into DMAc to form a solution of 20 wt%, which was spread on a horizontal glass plate by using a glass rod wrapped and placed on a hot platform step up from 60 to 120 °C for 12 h. The polymer film was obtained after drying in a vacuum oven at 200 °C for 24 h. The mechanical properties of the polymers were measured using the film (50 mm × 10 mm) stretching method in the Instron-3366 machine. An appropriate amount of the polymer was placed into the mold of the hot press, and then pressed at 320 °C for 40 min. The resulting sheets were cut into standard dimensions for determing their impact strengths. The optical properties of the films were characterized by a UV spectrophotometer(UV-2600). The thickness of the films was 60 μm and the test wavelength was in the range from 800 to 200 nm.

3 Results and discussion

3.1 Cloud point equation plotting

The composition and mass fractions at the cloud point was shown in Table 1. The turbidity plots of the three PEK-C/DMAc/NSA systems were obtained by linear fittingof the results of the cloud point titration. The LCP fittings of the cloud point data of the PEK-C/DMAc/NA systems are illustrated in Fig. 2 and Table 2. It was found that the turbidity points of the three systems conform to the LCP linear turbidity point equation, which the linear correlation coefficients not less than 0.997. The ternary phase diagrams can be obtained from the linear fitting equation, which for all the three systems are shown in Fig. 3. The absolute value of A in the equation reflected the change in the size of the homogeneous region in the ternary phase diagram, with the larger the absolute value of A, the smaller was the homogeneous region. The size of the homogeneous zone could reflect the solidification effect of the coagulant, $H_2O > EtOH > EA$. In the PEK-C/DMAc/EA system, the quality score of EA could reach 50%.

3.2 Analysis of molecular weight and PDI

Table 3 shows the results of the gradual precipitation fractionation of PEK-C with different poor solvents, and lists the doses of the poor solvents, precipitated weight in percentage, number-average molecular weight, weight-average molecular weight, PDI index, and characteristic viscosity of each grade.

Table 3 The results of gradual precipitation fractionation of PEK-C with different poor solvents

No	Poor solvent dosage(mL)	W (%)	Mn (kDa)	Mw (kDa)	PDI	η (dL/g)	Yield(%)
1	0	100	39	71	1.796	0.400	77.60
1–1	76	10.2	78	127	1.626	0.636	
1–2	1	20.0	68	96	1.424	0.563	
1–3	2	13.6	59	78	1.333	0.505	
1–4	3	11.2	52	65	1.254	0.437	
1–5	3	8.8	39	49	1.232	0.423	
1–6	Rotary evaporator	13.8	21	31	1.505	0.259	
2–1	345	13.8	79	123	1.541	0.619	83.40
2–2	10	14.6	73	102	1.403	0.565	
2–3	10	15.2	60	79	1.313	0.498	
2–4	10	9.0	54	67	1.236	0.444	
2–5	Rotary evaporator	22.8	27	38	1.429	0.211	
2–6	Centrifugation	8.0	17	24	1.43	0.280	
3–1	1350	8.2	113	158	1.400	0.694	83.40
3–2	75	11.6	97	126	1.288	0.607	
3–3	125	17.2	80	98	1.221	0.537	
3–4	225	15.2	65	77	1.185	0.460	
3–5	250	8.8	52	59	1.134	0.397	
3–6	Rotary evaporator	22.4	25	34	1.366	0.227	
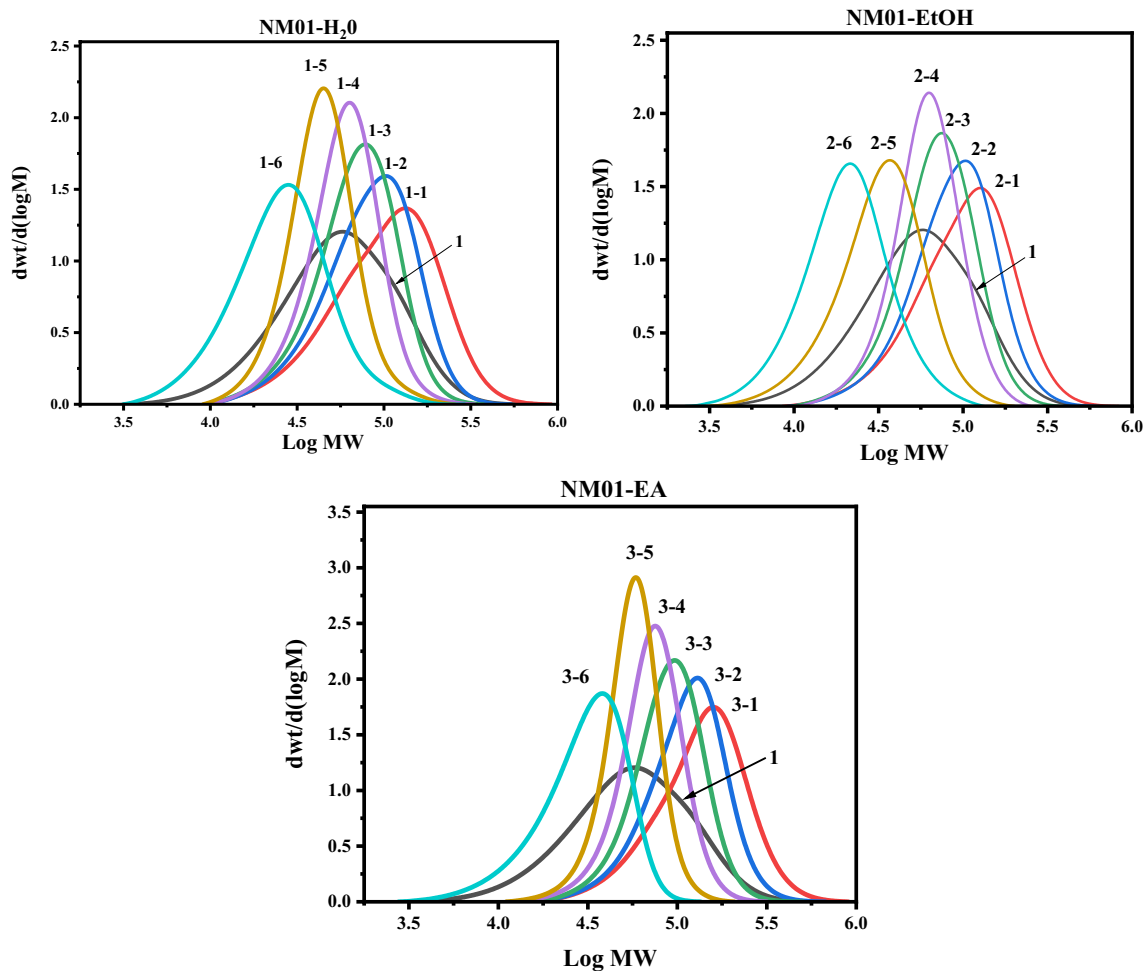
Fig. 4 Molar mass differential curves of PEK-C when different solutions are used as poor solvents

It can be seen from the molecular weight of PEK-C, which started at 39 kDa, and the first grade had the highest molecular weight, which can add up to 113 kDa once the poor solvent was added. With the addition of the poor solvents, the molecular weight of each grade decreased gradually. The molar mass differential curves of PEK-C, obtained by using different solutions as the poor solvents, are shown in Fig. 4. It can be seen that compared with the raw material of PEK-C, the peak shape of the distribution curve gradually narrows.

This was consistent with the basic principle of the incremental poor solvent fractionation method. In terms of the intrinsic viscosity, both viscosity and molecular weight of each grade showed a gradually decreasing trend.

On the one hand, through thequantity of the poor solution, it can been seen clearly that different poor solvent of precipitation effect is also different. The effecct of the precipitation of H_2O was greater than those of EtOH, and EA. Adding a small amount of H_2O in the process of fractionation can already achieve the result of fractionation, but EtOH and EA were needed to add a large amount of poor solvent. On the other hand, the weakly precipitated EA could be separated from the polymers to obtain smaller PDI (as low as 1.134) and narrower PDI. Meanwhile, EA also could get the highest molecular weight grade (113 kDa). Besides, by

applying the previous linear fitting equation, the amount of the added non-solvent could be calculated theoretically. For example, in the PEK-C/DMAc/H_2O system, 75.64 mL of H_2O was needed to reach its cloud point. While in the actual experiment, 76 mL was enough, which was very close to the theoretical one. Again, in the PEK-C/DMAc/EA system, 1280 mL EA was needed to reach its cloud point, while 1350 mL was added in the actual experiment. This happened mainly due to the fact that when the system just reached the cloud point, the amount of the precipitated polymer was too small to obtain by direct static precipitation. This required to keep adding EA, although its saturated vapor pressure was very low and easily volatilized during the dropwise addition. It eventually led to an increase in the EA dose.

When EA was used as a precipitator, the molecular weight distributed in the range of 25 ~ 113 kDa, PDI mostly distributed in the range of 1.1 ~ 1.4, the peak shape of 3–5 was the narrowest, and the PDI was 1.134. Its main reason was that when EA with weak precipitation effect was added to the solution, the dissolution balance in the system was broken, and the phase separation occured in an instant. At this moment, the least molecular weight species of polymer was precipitated, and the solvation effect and cohesion energy were the most similar. The concentration of the similar molecular weight was the highest, leading to the narrowest PDI. However, such narrow PDI cannot be obtained through condensation reactions.
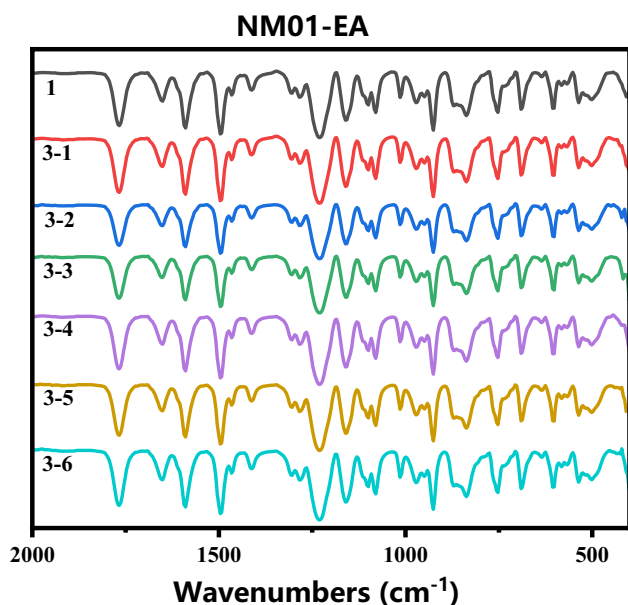

Fig. 5 The FT-IR spectra of the various grades in PEK-C/DMAc/EA system
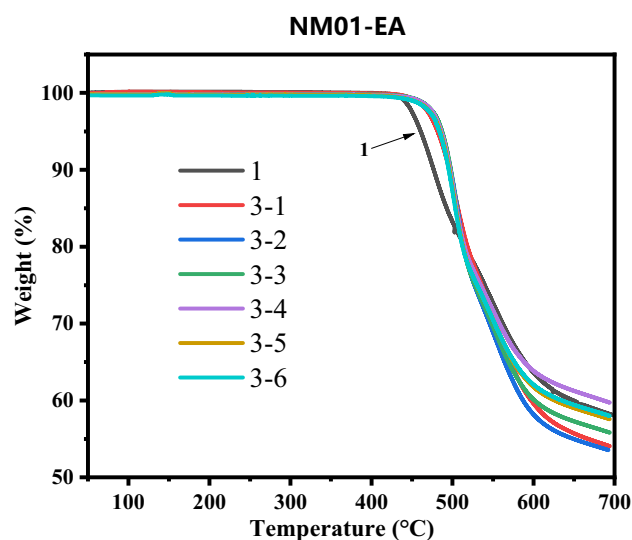

Fig. 6 TG curves of the various grades in PEK-C/DMAc/EA system

Table 4 $T_{d\,5\%}$ of the various grades in PEK-C/DMAc/EA system

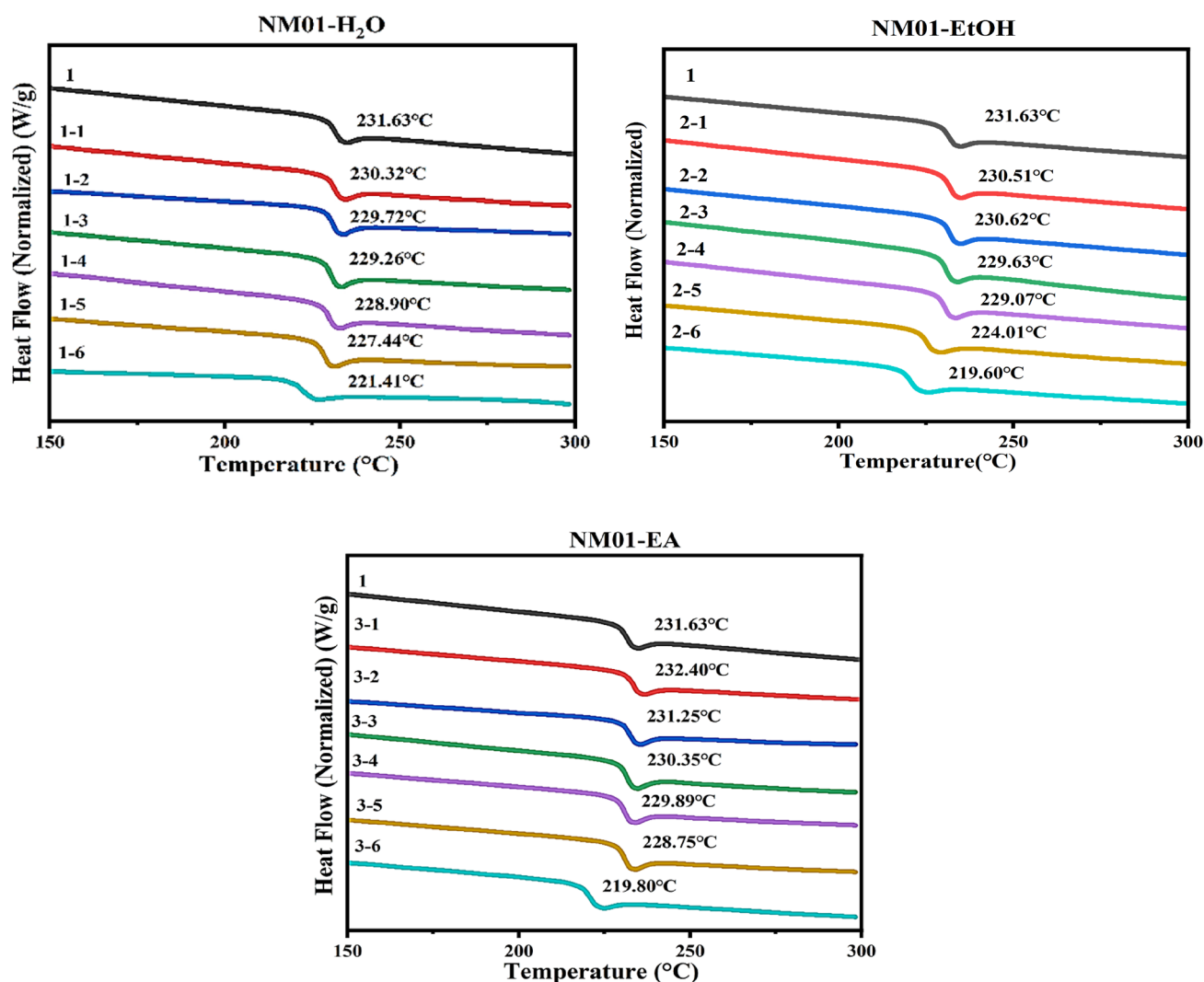| No	1	3–1	3–2	3–3	3–4	3–5	3–6
$T_{d\,5\%}$(°C)	460.7	481.6	486.2	487.2	486.0	484.6	483.8

Fig. 7 The secondary heating curve of each grade of DSC

By combining the grading method with the ternary phase diagram, the time required for adding the poor solvent could be reduced greatly, and the fractionation efficiency could also be improved. Besides, the use of EA as a poor precipitant could reduce the PDI of a polymer to a level that cannot be achieved through ordinary polycondensation reactions.

3.3 FTIR spectral analysis of each grade

Take various grades in PEK-C/DMAc/EA obtained as an example, infrared spectroscopy was used to characterize the chemical structures as illustrated in Fig. 5. The C=O stretching vibration peak of the ketone group at 1651 cm^{-1}, C=O stretching vibration peak on the ester group at 1774 cm^{-1}, vibrational bands of the benzene ring skeleton at 1597 cm^{-1} and 1500 cm^{-1}. And the 1230 cm^{-1} is the stretching vibration peak of Ar–O-Ar. The structure of the

polymer was identical to that of PEK-C as evidenced by the IR spectroscopy tests. The delivery grading of the precipitant did not change the structure of the polymer.

3.4 Analysis of thermal properties of grades

The thermal stabilities of various grades were evaluated by TGA as illustrated in Table 4 and Fig. 6. Few mass losses could be observed before 400 °C and carbon residue rate exceeded 50 °C at 700 °C. The thermal decomposition temperature for 5% mass loss remained at 460 °C ~ 488 °C, indicating excellent thermal stability. As seen, $T_{d\ 5\%}$ of the grades increased over 20 °C as the increase in the molecular weight led to the increase in the cohesion energy of the polymer, intermolecular forces, thermal stability, and $T_{d\ 5\%}$, such as 3-1, 3-2, 3-3. When the molecular weight was small, PDI was narrow, small molecule content was low, and the
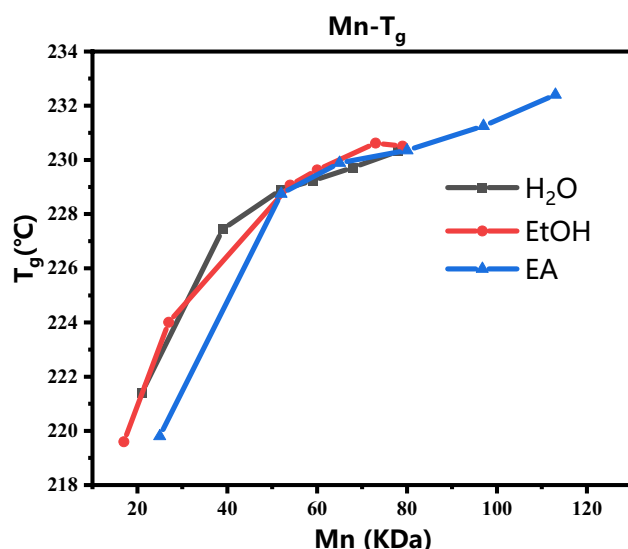
Fig. 8 Relationship between number average molecular weight of PEK-C and Tg
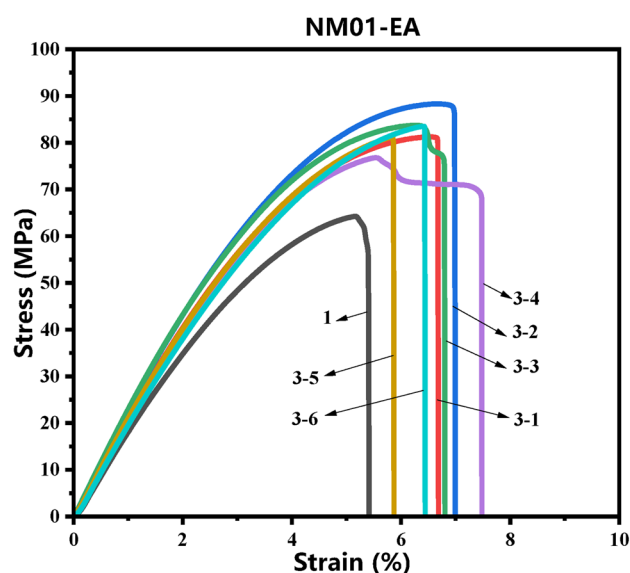

Fig. 9 Mechanical characterization parameters of PEK-C/DMAc/EA system

Table 5 Mechanical characterization parameters of different grades of PEK-C

No	Elastic modulus (Gpa)	Elongation at break (%)	Tensile strength (Mpa)
1	1.98	5.41	64.24
1–1	2.35	6.08	82.68
1–2	2.29	6.03	80.79
1–3	2.24	6.65	82.06
1–4	2.14	7.24	79.51
1–5	2.28	5.96	79.02
1–6	2.21	4.80	74.13
2–1	2.22	5.71	77.04
2–2	2.33	6.16	85.60
2–3	2.38	5.78	82.69
2–4	2.47	6.45	88.75
2–5	2.28	5.94	82.77
2–6	Broke		
3–1	2.25	6.69	81.26
3–2	2.40	6.99	88.31
3–3	2.38	6.80	83.73
3–4	2.15	7.48	76.78
3–5	2.21	5.87	81.20
3–6	2.11	6.43	83.51

amount of unstable end groups was reduced, making $T_{d\,5\%}$ of PEK-C higher, such as 3-4, 3-5, 3-6.

The second heating curves of different DSC grades are shown in Fig. 7. As can be seen from the figure, when H_2O, EtOH, and EA were used as poor solvents, T_g of each grade gradually decreased from 232 °C to 219 °C. Generally, T_g decreases with decrease in the molecular weight in a certain range. This can also be clearly seen from the relationship between the molecular weight and T_g in Fig. 8. When the molecular weight was less than 50 kDa, T_g increased greatly with increasing molecular weight, and changed slowly when the molecular weight is more than 50 kDa. This happened due to the fact that as the molecular weight increased, the degree of dispersion within the molecules and intermolecular interactions also increased. Therefore, when the molecular weight increased, the molecular motion decreased and the polymer cooled down slowly, which increased T_g. After the molecular weight reached a certain level, T_g had little relationship with the molecular weight, T_g depends more on the molecular structure and intermolecular forces.

The obtained mechanical properties of each grade are shown in Table 5 and Fig. 9. Since he molecular weight and PDI together determine the mechanical properties of polymers. After grading, the first few grades, such as 1-1, 2-1, 3-1, were found to have large molecular weights and wide PDIs, while the latter grades, such as 1-5, 2-5, 3-5, had small molecular weights and narrow PDIs. So,it was difficult to find the pattern from the molecular weight or PDI alone. However, it was seen from 3-3, 3-4 that the fracture mode of PEK-C could be changed from brittle to yield by regulating its molecular weight and PDI, It was also seen that PEK-C could not form an intact film when its molecular weight was below 19 kDa. Still it was found from the figure that the maximum elastic modulus, elongation at breaks and fracture strength of the grades were increased by 22.6, 38.3

Table 6 Mechanical characterization parameters of different grades of expanded PEK-C

No	W (%)	Mn (kDa)	Mw (kDa)	PDI	H (dL/g)	Yield (%)	Impact strength (KJ/m²)
1	100	39	71	1.80	0.400		5.1
K-1–1	71.7	64	103	1.60	0.536	95.4	5.9
K-1–2	71.4	29	46	1.57	0.340		5.2
K-2–1	39.0	65	114	1.76	0.660	79.0	7.2
K-2–2	79.5	38	64	1.68	0.423		5.6
K-3–1	51.9	61	92	1.50	0.535	88.3	6.9
K-3–2	80.5	36	64	1.79	0.354		5.4
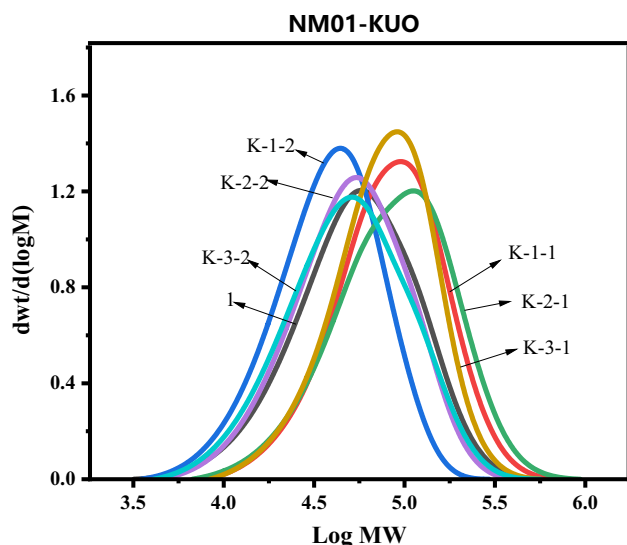
Fig. 10 Molar mass differential curve of PEK-C in enlarged fractionation
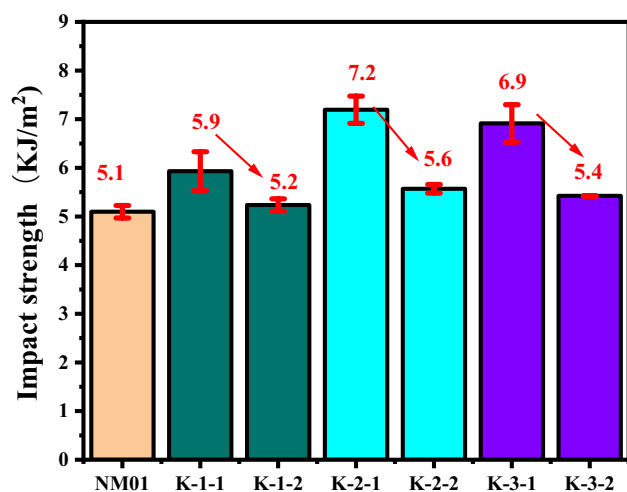
Fig. 11 Impact strength of different grades

and 38.2%, respectively. The elongation of the polymer at breaks was the maximum at the fourth grade.

In the process of fractionating by adding poor solvents, EA was used as a poor solvent to fractionate the solution with a relatively high concentration, due to its weak precipitation strength and good grading effect. One hundred gram of PEK-C was dissolved in the DMAc solution to obtain 10% solid concentration. EA was added drop by drop until the first grade appeared. Then, it was removed and diluted as the bottom solution. The first several grades were mixed and named as grade K-1, and then the remaining solution was collected after rotating evaporation and named as grade K-2. We can scale up production up to 70 g of PEK-C with high molecular weight and narrow PDI. The obtained results are shown in Table 6. As can be seen from Fig. 10, the raw polymer was divided into two grades with different molecular weights, with all the corresponding PDIs narrower than that of the raw material. It was in line with the conclusion derived by Whitfield. [50] Any PDI between two types of PDIs could be obtained by blending, maintaining a unimodal distribution.

After that, the parts were mixed to test the impact strength of the platen, whose obtained results are shown in Table 6 and Fig. 11. It can be seen that after fractionation, the impact strengths of both grades were bigger than that of the raw material. The impact strength of the polymer with a large molecular weight was large, and that of the polymer with a small PDI was also large. As the molecular weight increased, the molecular chains became longer and their intermolecular interactions were strengthened. Meanwhile, a narrower PDI led to the reduction in the roughness of the material surface during the processes of molding and improvement of the mechanical properties. As seen in the figure, K-1–3 could increase the impact strength by 41.2%. Through the method of adding precipitant, the impact strength of the polymer could be improved well.
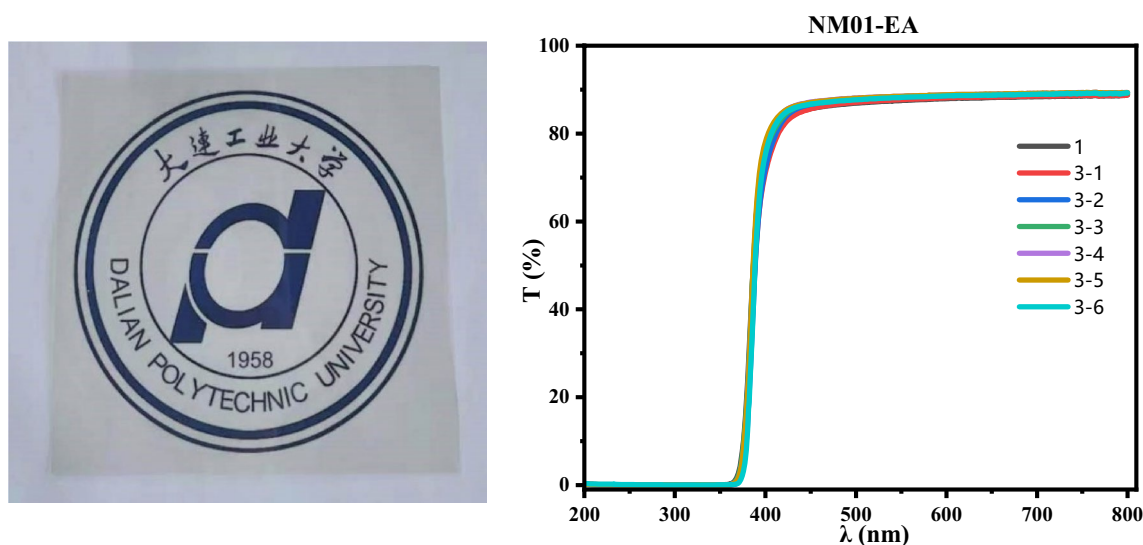
Fig. 12 Photo of PEK-C film and UV–vis transmission spectra of the PEK-C films

3.5 UV shielding performance of films of various grades

The optical properties of PEK-C with UV–vis are displayed in Fig. 12, which revealed that the transmittance of both polymers reached 85.6% at the wavelength of 450 nm, and the cut-off wavelength ($\lambda 0$) for PEK-C remained as 354.5 nm. It could be found that all the grades had good transmittance in the visible range, and at the same time they had good UV shielding properties also.

4 Conclusion

In conclusion, the ternary phase diagrams of three PEK-C/DMAc/NSA systems were analyzed by using the LCP linear cloud point equation. Among them, the PEK-C/DMAc/EA system could achieve the best results in the grading process. It was found that the ternary phase diagram could predict well the addition of non-solvent and improve the classification efficiency. It was also found that the maximum elastic modius, elongation and fracture strength of the films obtained after grading increased by 22.6, 38.3 and 38.2% for each grade, respectively. The effects of the molecular weight and PDI on the impact strength of polymer sheets were also investigated by using the expanded the fractionation method. The obtained results showed that the impact strength of each component was improved by increasing the molecular weight and decreasing the PDI, with the maximum improvement of 41.2%. Based on incremental poor solvent fractionation method, narrowly distributed polymers with better mechanical properties than the raw materials were obtained. The insight obtained from this paper can offer valuable references to the processing technique to obtain PEK-C with high molecular weight and narrow PDI.

References

1. N. Corrigan, C. Boyer, Macromolecules **55**, 8960 (2022)
2. B.K. Jang, M.H. Kim, O.O. Park, Macromol. Res. **28**, 343 (2019)
3. A.A. Higazy, H. Afifi, A.H. Khafagy, M.A. El-Shahawy, A.M. Mansour, Ultrasonics **44**, e1439 (2006)
4. E. Triwulandari, W. Fatriasari, A.H. Iswanto, M. Septiyanti, E.F. Umam, M. Ghozali, J. Mater. Res. Technol **19**, 2204 (2022)
5. F. Rao, Y. Ji, Y. Huang, N. Li, Y. Zhang, Y. Chen, W. Yu, Constr. Build. Mater. **292**, 123458 (2021)
6. T. Kida, R. Tanaka, Y. Hiejima, K.-H. Nitta, T. Shiono, Polymer **218**, 123526 (2021)

7. T. Siritientong, P. Aramwit, Macromol. Res. **23**, 861 (2015)

8. S.I. Rosenbloom, J.H. Hsu, B.P. Fors, J. Polym. Sci. **60**, 1291 (2022)

9. C. Long, Z. Dong, X. Liu, F. Yu, Y. Shang, K. Wang, S. Feng, X. Hou, C. He, Z.-R. Chen, Polymer **258**, 125287 (2022)

10. A.M. El Nahrawy, A.B.A. Hammad, A.M. Youssef, A.M. Mansour, A.M. Othman, Appl. Phys. A, 125 (2019).

11. A.M. El Nahrawy, A.B. Abou Hammad, A.M. bakr, T.I. Shaheen, and A.M. Mansour, Appl. Phys. A, 126 (2020).

12. A.M. El Nahrawy, A.S. Montaser, A.M. Bakr, A.B. Abou Hammad, A.M. Mansour J. Mater. Sci. Mater. Electron. **32** 28019 (2021).

13. J.Y. Guan, X. Zhang, Z.M. Ma, M. Xu, Plast. Rubber Compos. Process. Appl. **15**, 183 (1991)

14. D.R. Wiff, M. Gehatia, A. Wereta, J Polym Sci Pt B-Polym Phys. **13**, 275 (1975)

15. N.P. da Silva Chagas, G. Lopes da Silva Fraga, and M.d.F.V. Marques, Macromol. Res., **28**, 1082 (2020)

16. H.J. Cho, Y.J. Yoo, J.W. Kim, Y.H. Park, D.G. Bae, I.C. Um, Polym. Degrad. Stab. **97**, 1060 (2012)

17. J. Zhou, Q. Wang, C. Jia, M.T. Innocent, W. Pan, H. Xiang, M. Zhu, Macromolecules **54**, 7529 (2021)

18. J. Roovers, J.D. Cooney, P.M. Toporowski, Macromolecules **23**, 1611 (1990)

19. J.K. Fink, *High Perform. Polym*, 153 (2014).

20. F. Liu, Z. Wang, H. Wang, G. Zhou, S. Cui, J Functional Polymer **27**, 99 (2014)

21. M. Xie, M. Yin, G. Nie, J. Wang, C. Wang, D. Chao, X. Liu, J Polym Sci Part A: Polym Chem **54**, 2714 (2016)

22. C. Wu, M. Siddiq, S.Q. Bo, T.L. Chen, Macromolecules **29**, 3157 (1996)

23. C. Yu, J. Sang, Y. Li, T. Li, L. Yan, Z. Zhang, Polymer Materials Science Engineering **31**, 16 (2015)

24. C. Wu, S.Q. Bo, M. Siddiq, G.J. Yang, T.L. Chen, Macromolecules **29**, 2989 (1996)

25. M. Siddiq, C. Wu, M. Nawaz, M.K. Baloch, K. Mahmood, B. Mohammad, J. Chem. Soc. Pak. **23**, 200 (2001)

26. S.X. Zheng, K.M. Nie, Q.P. Guo, Thermochim. Acta **419**, 267 (2004)

27. J. Peng, Q. Wang, J. Wang, J. Yang, T. Jiang, G. Zeng, Macromol. Res. **30**, 826 (2022)

28. Q. Wang, S. Zhang, F. Dai, X. Yan, G. Qian, C. Chen, Y. Yu, J. Environ. Chem. Eng. **9**, 106132 (2021)

29. M. Ling, K. Yu, J. Wang, H. Wang, H. Nie, Z. Wang, G. Zhou, Thermochim. Acta. **714**, 179253 (2022)

30. M. Garcia-Leiner, M.T.F. Reitman, M.J. El-Hibri, R.K. Roeder, Polym. Eng. Sci. **57**, 955 (2017)

31. Y. Shibasaki, T. Araki, R. Nagahata, M. Ueda, Eur. Polym. J. **41**, 2428 (2005)

32. M. Siddiq, C. Wu, B.Y. Li, J. Appl. Polym. Sci. **60**, 1995 (1996)

33. Y. Liu, S. Bo, Int. J. Polym. Anal. Charact. **8**, 225 (2010)

34. Y. Xue, S. Bo, and X. Ji, J. Polym. Res., **23** (2016).

35. Y.-H. Xue, S.-Q. Bo, X.-L. Ji, Chin. J. Polym. Sci. **33**, 1586 (2015)

36. P. Li, Y. Xue, X. Wu, G. Sun, X. Ji, and S. Bo, J. Polym. Res. **25** (2018).

37. A. Lehtinen, R. Paukkeri, Macromol. Chem. Phys. **195**, 1539 (1994)

38. L. Tan, Z. Huang, W. Hu, N. Xu, Q. Cao, M. Wang, J Solid Rocket Technol **38**, 893 (2015)

39. H. Choi, K. Im, T. Chang, Macromol. Res. **20**, 101 (2012)

40. A. Ndiripo, A. Albrecht, B. Monrabal, J. Wang, H. Pasch, Macromol. Rapid Commun. **39**, 1700703 (2018)

41. H. Huang, J. Zhang, L. Hou, D. Wei, W. Wang, M. Guo, Plastics **40**, 6 (2011)

42. M. Guo, J. Zhang, H. Huang, L. Hou, Q. Li, Petrochemical Technology **34**, 173 (2005)

43. S. Cheruthazhekatt, H. Pasch, Anal. Bioanal. Chem. **405**, 8607 (2013)

44. R.M. Boom, T. van den Boomgaard, J.W.A. van den Berg, C.A. Smolders, Polymer **34**, 2348 (1993)

45. F.W.S. Altena, C. A Macromolecules **15**, 1491 (1982)

46. G. Bakeri, A.F. Ismail, M. Rahimnejad, and T. Matsuura, J. Polym. Res. **21** (2014).

47. Y.M. Wei, Z.L. Xu, X.T. Yang, H.L. Liu, Desalination **192**, 91 (2006)

48. L. Xu, F. Qiu, Polymer **55**, 6795 (2014)

49. C.Q. Yin, J. Dong, Z.T. Li, Z.X. Zhang, Q.H. Zhang, Polym. Bull. **72**, 1039 (2015)

50. R. Whitfield, N.P. Truong, A. Anastasaki, Angew. Chem. Int. Ed. **60**, 19383 (2021)

Authors and Affiliations

Zengxu Qian[1] · Jingwei Jiang[1] · Yunlong Sun[2] · Qiliang Yuan[3] · Zhichao Wang[1] · Zhipeng Wang[2] · Guangyuan Zhou[2]

✉ Zhichao Wang
wangzc@dlpu.edu.cn

✉ Zhipeng Wang
okko@dicp.ac.cn

[1] School of Textile and Material Engineering, Dalian Polytechnic University, Dalian 116034, China

[2] Division of Energy Materials (DNL22), Dalian Institute of Chemical Physics of the Chinese Academy of Sciences, Dalian 116023, China

[3] Zhejiang Zhongxin Fluoride Materials Co., Ltd., Shaoxing City 312369, China